Magnetization reversal and magnetic anisotropies in epitaxial Fe/MgO and Fe/MgO/Fe heterostructures grown on Si(001)

C. Martínez Boubeta[a] and A. Cebollada
Instituto de Microelectrónica de Madrid–IMM (CNM–CSIC), Isaac Newton 8, PTM, E-28760, Tres Cantos, Madrid 28760, Spain

J. F. Calleja and C. Contreras
Departamento de Física, Laboratorio de Magneto-Optica, Universidad de Oviedo, Calvo Sotelo s/n, E-33007 Oviedo, Spain

F. Peiró and A. Cornet
Electronic Materials and Engineering, Facultat de Fisica, Universitat de Barcelona, Avinguda Diagonal 645-647, E-08028 Barcelona, Spain

(Received 7 October 2002; accepted 24 November 2002)

Epitaxial Fe/MgO heterostructures have been grown on Si(001) by a combination of sputtering and laser ablation deposition techniques. The growth of MgO on Si(001) is mainly determined by the nature of the interface, with large lattice mismatch and the presence of an amorphous layer of unclear origin. Reflection high energy electron diffraction patterns of this MgO buffer layer are characteristic of an epitaxial, but disordered, structure. The structural quality of subsequent Fe and MgO layers continuously improves due to the better lattice match and the burial of defects. A weak uniaxial in-plane magnetic anisotropy is found superimposed on the expected cubic biaxial anisotropy. This additional anisotropy, of interfacial nature and often found in Fe/MgO and Fe/MgO/GaAs(001) systems, is less intense here due to the poorer MgO/Si interface quality compared with that of other systems. From the evolution of the anisotropy field with film thickness, magnetic anisotropy is also found to depend on the crystal quality. Kerr measurements of a Fe/MgO multilayered structure grown on Si show two different switching fields, suggesting magnetic coupling of two of the three Fe layers. Nevertheless, due to the little sensitivity to the bottom Fe film, independent switching of the three layers cannot be ruled out. © *2003 American Institute of Physics.* [DOI: 10.1063/1.1538317]

I. INTRODUCTION

The fabrication of single crystalline structures composed of metallic, semiconducting and insulating materials with some, or all of them, of ferromagnetic nature opens up a wide range of fields of research and the exploration of new phenomena that are highly relevant from the fundamental and technological points of view. This is clearly exemplified by novel disciplines like magnetoelectronics or spintronics,[1] due to their exploitation of the spin character of the electron in electronic devices. To mention just one example, the investigation of magnetic tunnel junctions with potential applications in magnetic random access memory (MRAM) devices has been in recent years one of the most active fields of research within these areas.[2]

On the other hand, the availability of single crystalline magnetic heterostructures with atomically abrupt interfaces allows understanding many fundamental properties of magnetism in solid state physics. These heterostructures are highly desirable, especially regarding the study of properties that can often be extremely defect and interface sensitive, like in the case of the magnetic anisotropy.[3] If these magnetic heterostructures are grown on a semiconductor, this also opens up new directions for the potential integration of high density storage media and magnetic sensor devices in the present day semiconductor technology available.

Different semiconductor materials have been selected as substrates for the fabrication of magnetic heterostructures depending of their specific properties, such as lattice mismatch, crystalline quality, thermal stability, electron mobility, etc. In the case of Si, an additional advantage over other semiconductors is that it is the most widely used substrate in conventional semiconductor technology, and as a consequence the price of high quality single crystals of this material is moderate and most technological processes are specifically optimized for it.

There is plenty of work that treats the epitaxy and magnetic properties of metals grown on semiconductor substrates, e.g., Waldrop and Grant's[4] and Prinz and co-workers' [5,6] pioneering work on the epitaxial growth of Fe on GaAs. In the case of Si, Chang demonstrated the epitaxial growth of a wide variety of metals on Si(001) using different metallic seed layers.[7] Nowadays, many research groups follow the procedures used in earlier work to obtain epitaxial metallic ferromagnetic thin films using high quality semiconductor substrates. Nevertheless, problems like strong metal/semiconductor intermixing and usually high mismatch between $3d$ ferromagnetic layers and substrates suggest the use of alternative buffer layers. MgO has often been selected

[a]Electronic mail: boubeta@imm.cnm.csic.es

 © 2003 American Institute of Physics

Downloaded 11 Jun 2010 to 161.116.168.169. Redistribution subject to AIP license or copyright; see http://jap.aip.org/jap/copyright.jsp

for this (see, for example, Refs. 8–10), because it has shown excellent properties as a diffusion barrier with thermal stability up to 800 °C and significant good electrical insulation characteristics in layered systems.[11]

MgO is a highly ionic material with a NaCl structure. It has face-centered-cubic (fcc) Mg and O sublattices, and low energy {100} cleavage surfaces. Both the high mismatch of -22.5% between MgO (lattice constant $a_{\mathrm{MgO}}=4.21$ Å) and Si (lattice constant $a_{\mathrm{Si}}=5.43$ Å) and the large difference in thermal expansion coefficients ($\alpha_{\mathrm{MgO}}=13.5\times10^{-6}/°\mathrm{C}$ vs $\alpha_{\mathrm{Si}}=4\times10^{-6}/°\mathrm{C}$) in principle make the epitaxy of MgO on Si(001) quite unlikely. As a consequence, there are few publications in which MgO/Si epitaxy is treated, either by laser ablation[9,12–15] or other deposition techniques.[16]

First studied almost 30 years ago[17,18] the epitaxy and magnetic properties of the Fe(001)/MgO(001) system have received a lot of attention since then and nowadays can be considered a model system for the study of many fundamental magnetic properties. It follows the Fe(001)[110]‖MgO(001)[100] epitaxial relation helped by the relatively low lattice mismatch (3.8%) upon 45° in plane rotation. Because of the lack of electronic interaction at the Fe–MgO (001) interface, the electronic and magnetic properties of an atomic layer of Fe on top of MgO(001) have theoretically been predicted to be remarkably close to those of a free-standing Fe monolayer,[19] thereby being an attractive two-dimensional (2D) system with which to carry out interface anisotropy studies.

Magnetic anisotropies have been intensively studied in the Fe/MgO system,[20–25] with important contributions of interfacial nature in many cases. Much more recently, the Fe/MgO/Fe system has also been used for the study of tunnel magnetoresistance in fully epitaxial tunnel junctions[26,27] as well as for exchange interactions between two ferromagnets through an insulator.[28]

In previous work we performed a complete study of the epitaxy, magnetic anisotropies and magnetization reversal processes of Fe(001) thin films grown directly on bulk MgO(001) or on MgO buffered GaAs (001) substrates.[29–34] In this paper we extend our previous work and present our results on the epitaxy and magnetic properties of Fe/MgO heterostructures, both in single layer and multilayered form, on Si(001) substrates.

II. EXPERIMENTAL PROCEDURE

The structures were grown on Si(001) substrates (0° off). To obtain a hydrogen terminated oxide free Si(001) surface, the substrates were first dipped into an ultrasonic methanol bath for 40 s, followed by dipping for 40 s into a H_2SO_4 (10%) solution and then rinsed in another ultrasonic methanol bath for 40 s. Finally, the substrates were dipped into a solution of HF (10%) for 40 s. In looking for an ideal 1×1 dihydride structure, it should be noted that the Si substrates after the final HF cleaning were not subjected to subsequent rinsing with ultrapure water to avoid changes in surface structure that would lead to the appearance of 2×1 reconstruction.[35] The substrates were then loaded into a growth chamber with 2×10^{-9} mbar base pressure, and annealed at 500 °C until a characteristic (1×1) Si(001) reflection high energy electron diffraction (RHEED) pattern was observed *in situ*.

Before Fe deposition, a 200 Å MgO buffer layer was grown at 450 °C by normal incidence pulsed laser deposition from a rotating single crystalline MgO target in the pressure range of 7×10^{-9} mbar, described elsewhere.[31] This MgO layer provides not only an appropriate seed layer for the epitaxy of body-centered-cubic (bcc) Fe(001) films, but also serves as a diffusion barrier for Si substrate atoms in the Fe overlayer that might alter the magnetic behavior of the $3d$ metal.[36] Onto this MgO buffer layer, Fe films were deposited by normal incidence triode sputtering at 4×10^{-4} mbar Ar pressure. Further depositions of MgO and/or Fe were performed under the previously described conditions. To prevent the films from oxidation, all structures fabricated were terminated with a 25 Å Pt capping layer deposited by sputtering at room temperature (RT). For both the laser ablation and the sputtering cases, the deposition rates (0.1–0.2 Å/s) were calibrated by a profilometer and transmission electron microscopy (TEM) measurements.

The structure was checked *ex situ* by x-ray diffraction (XRD) using Cu $K\alpha$ radiation ($\lambda=1.5418$ Å), a Bragg–Brentano configuration, a secondary Cu monochromator and 1/4° slits. The surface morphology was examined by atomic force microscopy (AFM), which scanned areas of up to $10\times10\ \mu\mathrm{m}^2$. Some specific structures were also studied by TEM.

With regard to magnetic characterization, in-plane $M-H$ loops were measured *ex situ* by the magneto-optical Kerr effect (MOKE) in transverse geometry at RT. A magnetic field was applied in the film plane and swept at a frequency of ~2 Hz using Helmholtz coils. The direction of the field applied was fixed perpendicular to the plane of incidence, and the angle of incidence was 60°. A polarized laser source operating at 634.8 nm was used together with a photodiode detector in order to measure changes in the amplitude of the reflectivity.

Magnetization processes and magnetic anisotropies, on the other hand, were studied using transverse biased initial susceptibility (TBIS) experiments.[34] This technique basically consists of the application of a small alternating magnetic field h and an orthogonal steady field H both in the film plane. The Kerr signal is proportional to the component of the magnetization parallel to h (ΔM). If the amplitude of h is sufficiently small, ΔM will be proportional to the transverse susceptibility defined as $\chi_t=\mathrm{d}M_t/\mathrm{d}h$, where M_t is the component of saturation magnetization along alternating field h. Linear extrapolations of χ_t^{-1} for high H values would lead to anisotropy field H_k.

III. GROWTH AND STRUCTURAL CHARACTERIZATION

In this work, results will be presented for three different samples with the following nominal structures: 25 Å Pt (RT)/300 Å Fe (RT+anneal at 400 °C)/200 Å MgO (400 °C)/Si(001), 25 Å Pt (RT)/200 Å Fe (400 °C)/300 Å Fe (RT+anneal at 400 °C)/200 Å MgO (400 °C)/Si(001) and 25 Å

Downloaded 11 Jun 2010 to 161.116.168.169. Redistribution subject to AIP license or copyright; see http://jap.aip.org/jap/copyright.jsp

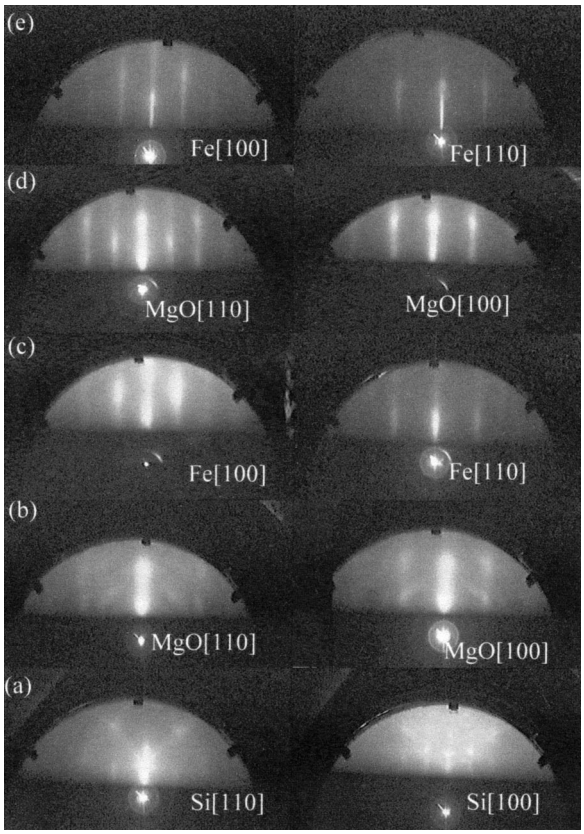

FIG. 1. RHEED patterns along two different azimuths taken during deposition of the Fe/MgO multilayered structure on Si(001): (a) Si(001) substrate; (b) 200 Å MgO buffer layer; (c) 300 Å Fe grown at RT and annealed at 400 °C; (d) 20 Å MgO; (e) 200 Å Fe grown at RT and annealed at 400 °C.

Pt (RT)/100 Å Fe (RT+anneal at 400 °C)/20Å MgO (400 °C)/200 Å Fe (RT+anneal at 400 °C)/20 Å MgO (400 °C)/300 Å Fe (RT+anneal at 400 °C)/200 Å MgO (400 °C)/Si(001). For the sake of simplicity, these will be called as single Fe layer structure, a double Fe layer structure and a Fe/MgO multilayered structure, respectively.

In Fig. 1 we show RHEED patterns of different steps in the fabrication of a multilayered Fe/MgO structure on Si(001), confirming the epitaxial Fe(001)[110]// MgO(001)[100]//Si(001)[100] orientation. Figure 1(a) shows the Si(001) substrate after the cleaning procedure and annealing at 500 °C. The diffraction pattern of the MgO buffer layer after deposition at 400 °C is shown in Fig. 1(b). The diffraction streaks are intense but broad, some of them with a ring shape, indicative of highly textured, but defective, growth. This can be understood by taking into account the large lattice mismatch between MgO and Si (−22.5%). This quality also compares unfavorably with that of MgO grown on GaAs(001), where we have observed sharp intense diffraction streaks for MgO grown under equivalent deposition conditions,[31] in spite of the very similar lattice mismatch. Obviously different cleaning procedures and surface preparations [*in situ* arsenic cap desorption for GaAs(001) versus *ex situ* HF cleaning for Si(001)], as well as interface chemistry between the semiconductor and insulator could explain the difference in quality between the MgO/GaAs and MgO/Si epitaxies.

Figure 1(c) shows RHEED patterns of a 300 Å Fe thin film on top of the MgO buffer layer. Fe films were grown at RT and annealed at 400 °C. This low deposition temperature reduces surface diffusion and therefore the natural tendency of Fe to grow on MgO by simultaneous three-dimensional (3D) growth,[37] while the ulterior annealing improves crystalline quality and surface roughness.[31] The RHEED patterns confirm the epitaxial relation previously described. The next step in the fabrication of a Fe/MgO multilayered structure was the deposition of a 20 Å MgO film on Fe at 400 °C. The quality of the diffraction pattern [Fig. 1(d)] is much better than that obtained for the MgO buffer layer [Fig. 1(b)]. The diffraction streaks are now sharper and more intense, with the symmetry being equivalent to that of the MgO buffer layer. This improvement in structure can be easily understood by taking into account the respective lattice mismatches between MgO and Fe (3.8%) or Si (−22.5%). Obviously, due to the much lower lattice mismatch, the MgO/Fe interface has a much higher degree of crystalline coherency compared with the MgO/Si one, and therefore, the crystal quality of MgO is higher when grown on Fe than when grown on Si under identical experimental conditions. As a result, crystalline quality enhancement of successive Fe layers would also be expected as long as each MgO thin film is improved with respect to previously deposited ones. This is corroborated in Fig. 1(e) where the RHEED pattern for the next Fe film grown at RT and annealed at 400 °C exhibits sharp intense diffraction streaks with much lower background compared with previous Fe films. This sequence of RHEED patterns provides evidence of the possibility of growing epitaxial Fe/MgO heterostructures on Si substrates, because it shows a clear improvement in the structural quality as the number of stacks increases.

With regard to the morphology of the final structure, AFM measurements were taken *ex situ* for the different samples. In the case of the single Fe layer structure, a root mean square (rms) roughness of 8 Å was obtained, which is more than double the 3 Å measured for Fe films grown under identical conditions on MgO/GaAs(001) surfaces.[31] For the case of the double Fe layer structure, AFM inspection revealed an increase in rms roughness of 30 Å. This was previously observed, for example, by Thürmer *et al.*[38] and Family and Amar.[39] who have shown that pyramid-like structures with increased roughness result each time homoepitaxial Fe growth takes place at high temperatures.

Finally, in the Fe/MgO multilayered structure the rms roughness was 8 Å, the same as that obtained in the Fe individual layer grown at RT and annealed. This implies that the deposition of successive Fe and MgO layers under adequate conditions does not deteriorate the surface morphology of the final structure, with this lower roughness probably being due to the defective HF-cleaning process and to an imperfect epitaxy of the MgO buffer layer on Si(001).

Further structural characterization was performed by XRD *ex situ*. Figure 2 shows high angle XRD measurements that correspond to those of the Fe/MgO multilayered structure. The symmetric scans are separated into two regions where relevant reflections are observed. In Fig. 2(a), MgO(200) and Pt(200) reflections are shown. Whereas the

Downloaded 11 Jun 2010 to 161.116.168.169. Redistribution subject to AIP license or copyright; see http://jap.aip.org/jap/copyright.jsp

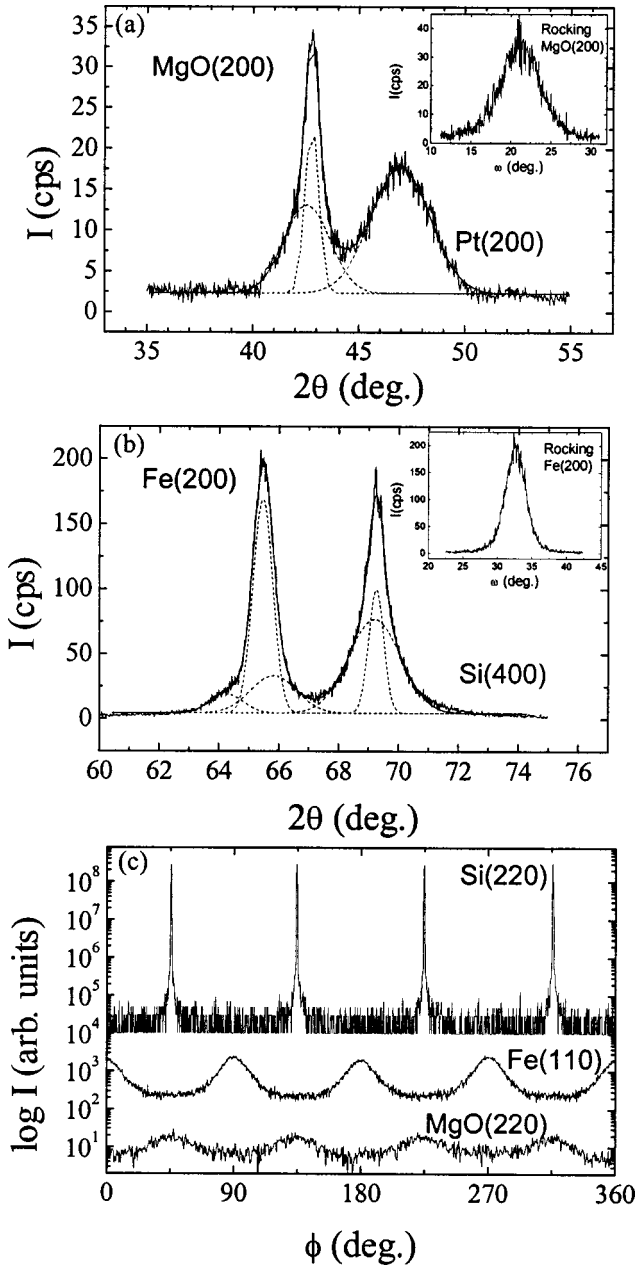

FIG. 2. High angle XRD pattern of the Fe/MgO multilayered structure: (a) MgO(200) and Pt(200) regions. Dashed lines are Gaussian fits. Inset: Rocking curve for the MgO(200) peak. (b) Fe(200) and Si(400) regions. Dashed lines are Gaussian fits. Inset: Rocking curve for the Fe(200) peak. (c) ϕ scans of MgO(220), Fe(110) and Si(220) asymmetric reflections. The curves are offset vertically for clarity.

diffraction peak corresponding to the Pt capping layer is symmetric, that corresponding to MgO exhibits clear asymmetry, as can be seen by fitting it to one and two Gaussian peaks, respectively. This asymmetry in the MgO peak is also observed in the other two structures fabricated, in which only one single MgO layer is present, and it cannot be attributed therefore as originating from the different MgO layers in the multilayered structure. This asymmetry is probably due to inhomogeneous strain present at the MgO/Si interface, or to MgO grains that are slightly rotated with respect to each other. In the inset of Fig. 2(a) the rocking curve corresponding to MgO(200) is also shown, and it has a 5.8° full width at half maximum (FWHM), indicative of a high mosaic spread. The other region of interest in the XRD symmetric scans is shown in Fig. 2(b), where both Fe(200) and Si(400) reflections are clearly observed. The low intensity of the Si peak is due to a small misalignment relative to the substrate introduced during the measurement, but it does not significantly alter the results of the epitaxial films. Si and Fe peaks are fitted to two and three Gaussians, respectively. Whereas the two Gaussian peaks used to reproduce substrate reflection do not have any physical meaning since the substrate is misaligned, this allows accurate background subtraction in the Fe(200) region, and therefore allows one to perform a confident fit of this layer peak (note the almost perfect agreement of the fit with the experimental data). The individual widths of these three peaks used to fit the Fe(200) reflection yield out of plane coherence lengths of 55, 75 and 125 Å, respectively, by use of the Scherrer equation, and could be attributed as originating from the individual 100, 200 and 300 Å Fe layers. Nevertheless, some degree of asymmetry is also observed in the other single and double Fe layered structures, and therefore assigning it to lattice distortion due to the presence of residual strain seems to be a more plausible interpretation of this result. In the inset of Fig. 2(b) the rocking curve of Fe(200) is also shown, and it yields a mosaic spread of 3.5°, better than that obtained for MgO, but twice the value obtained for similar films grown on MgO buffered GaAs(001).[32]

This improvement in mosaicity from MgO to Fe is easy to understand, since most of the intensity of the MgO(200) reflection comes from the 200 Å thick MgO buffer layer (the other two MgO films are only 20 Å thick), and therefore the mosaicity observed is mostly due to this first layer grown on Si, which exhibits an incoherent interface due to the very large lattice mismatch. On the other hand, the Fe(200) reflection is due to successive Fe layers grown on MgO, and it has a much lower lattice mismatch and crystalline quality which improves with the number of stacks as shown by RHEED. Finally, the in-plane crystalline order of the Fe/MgO multilayered structure can be further confirmed by taking asymmetric ϕ scans, which are shown in Fig. 2(c) for the MgO(220), Fe(110), and Si(220) reflections. Four characteristic peaks 90° apart demonstrate the cubic in-plane order of both the MgO and Fe individual layers. On the other hand, their relative orientation with respect to the Si(220) reflections further confirms that previously concluded by the RHEED epitaxial relation.

In order to corroborate some results assumed from the previous structural characterization techniques, the multilayered structure was examined by transmission electron microscopy. Figure 3(a) corresponds to a bright field cross-sectional view of the whole structure along the [1–10]Si zone axis orientation. The dark layers correspond to Fe and the brighter ones are MgO. According to TEM measurements the average thicknesses of the layers are somehow dissimilar from the nominal structure: 150 Å for the MgO buffer, 250 Å for the bottom Fe layer, 20 Å for the first MgO barrier, 160 Å for the medium Fe layer, 30 Å for the second MgO barrier and, finally, 60 Å for the topmost Fe layer and 35 Å Pt capping.

Downloaded 11 Jun 2010 to 161.116.168.169. Redistribution subject to AIP license or copyright; see http://jap.aip.org/jap/copyright.jsp

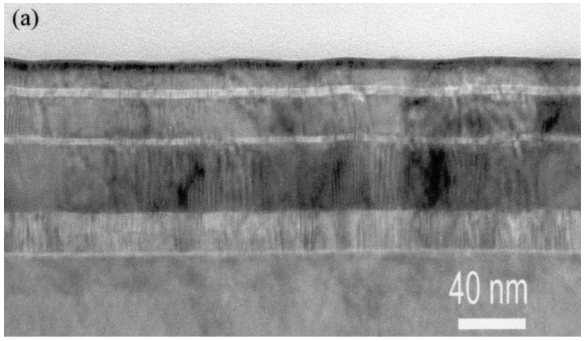

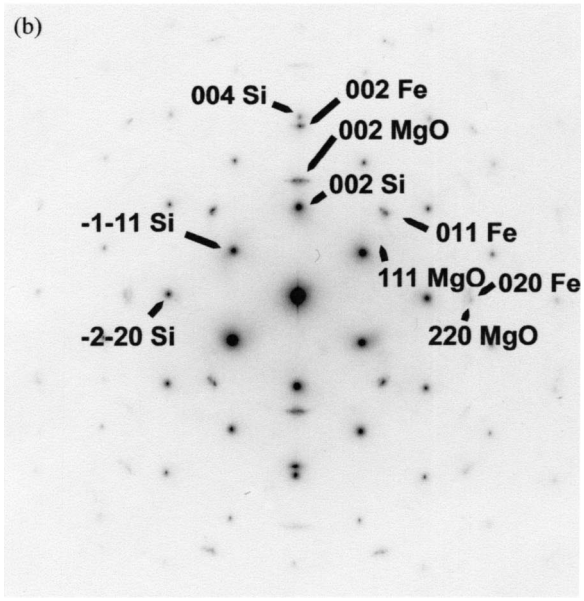

FIG. 3. (a) Cross-sectional TEM view of a Fe/MgO(001) multilayer along the [1-10]Si zone axis orientation. The dark layers correspond to Fe and the brighter ones are MgO. The presence of an amorphous layer, with a thickness of 15 Å, between the Si substrate and the MgO buffer can be seen. (b) Indexed electron diffraction pattern of the structure along the [1-10]Si axis demonstrating that, despite the amorphous layer over the Si substrate, the upper layers have grown epitaxially.

The presence of an amorphous layer, with thickness of 15 Å, between the Si substrate and the MgO buffer can be noticed. Since stoichiometry measurements were not performed, the nature of this amorphous layer remains unclear but it should be SiO_x coming from a defective HF-cleaning process, or amorphous MgO due to imperfect initial growth on Si(001).

Despite the presence of this layer, the MgO buffer has grown highly textured according to the relation MgO(001)[1−10]//Si(001)[1−10] in agreement with the *in situ* characterization by RHEED. This layer consists of grains that are slightly rotated one to the other with respect to the [1−10] axis, with deviation of the [001]MgO direction with respect to [001]Si of ±6°. This is also noticeable in Fig. 3(a) where some moiré fringes caused by overlapping of grains due to the thickness of the TEM foil are clearly visible. Rotation with respect to the [001] axis cannot be disregarded, but further analysis of plane-view or [110] cross-sectional orientations should be carried out by TEM to assess the mosaicity of the buffer.

The selected area diffraction pattern of the structure reveals that, despite the amorphous layer over the Si substrate, the upper layers have grown and follow the epitaxial relationship Fe(001)[110]//MgO(001)[100]//Si(001)[100] as illustrated in Fig. 3(b) obtained along the [100]Fe//[1−10]MgO//[1−10]Si zone axis.

The observation of the thin foil for several microns, under two beam diffraction conditions to enhance diffraction contrast, is evidence of rotated grains but it does not reveal the presence of pinholes in the MgO barriers. Moreover, the interfaces appear quite abrupt with no evidence of intermixing between the Fe and MgO layers. However undulation of the layers is observed in some regions. This undulation is a consequence of propagation of the roughness of the top surface of the MgO buffer.

IV. MAGNETIC PROPERTIES OF INDIVIDUAL Fe THIN FILMS

MOKE hysteresis loops were taken for the three samples described in this work. In Fig. 4(a) we show the loops that correspond to the single Fe layer structure, with H applied along different Fe crystallographic directions. Well defined rectangular hysteresis loops are observed when the magnetic field is applied along the [100] and [010] Fe directions, corresponding to magnetic easy axes. The normalized remanence M_r/M_s (where M_r is remanent magnetization and M_s is magnetization at saturation) amounts to 0.97, indicating that the Fe layer is essentially single domain in nature or even preferred domain orientations pointing along these easy axes. In this case, magnetization reversal takes place by nucleation and successive propagation of 180° domain walls.[30] Relatively low coercive field values of $H_c \approx 12$ Oe, very similar to the ones obtained for Fe/MgO (Ref. 30) and Fe/MgO/GaAs,[34] may be indicative of the good Fe crystalline quality due to the low number of pinning wall centers. In contrast, starting from the saturated state along the hard [110] axis, when the field strength is reduced the magnetization gradually decreases towards a value close to $M_s/\sqrt{2}$, and then suffers an irreversible jump at low negative field to $-M_s/\sqrt{2}$. This switching occurs at 45° with respect to the field direction, that is, a jump is expected to proceed via nucleation of domains oriented along the easy axis and rapid movement of 90° domain walls. By increasing the field's magnitude, the magnetization rotates continuously towards the field direction. A compilation of these results is given in Fig. 4(b), where the in-plane magnetic remanence as a function of the field angle applied with respect to Fe crystallographic directions is shown. This behavior clearly shows that the film displays fourfold in-plane magnetic anisotropy as expected for all Fe(001) films when evaporated perpendicular to the substrate surface[40] and it is qualitatively and quantitatively similar to that obtained in Fe(001) films grown on bulk MgO substrates.[30]

Finally, the double Fe layer structure exhibits in-plane biaxial anisotropy as in the former case, but with higher co-

Downloaded 11 Jun 2010 to 161.116.168.169. Redistribution subject to AIP license or copyright; see http://jap.aip.org/jap/copyright.jsp

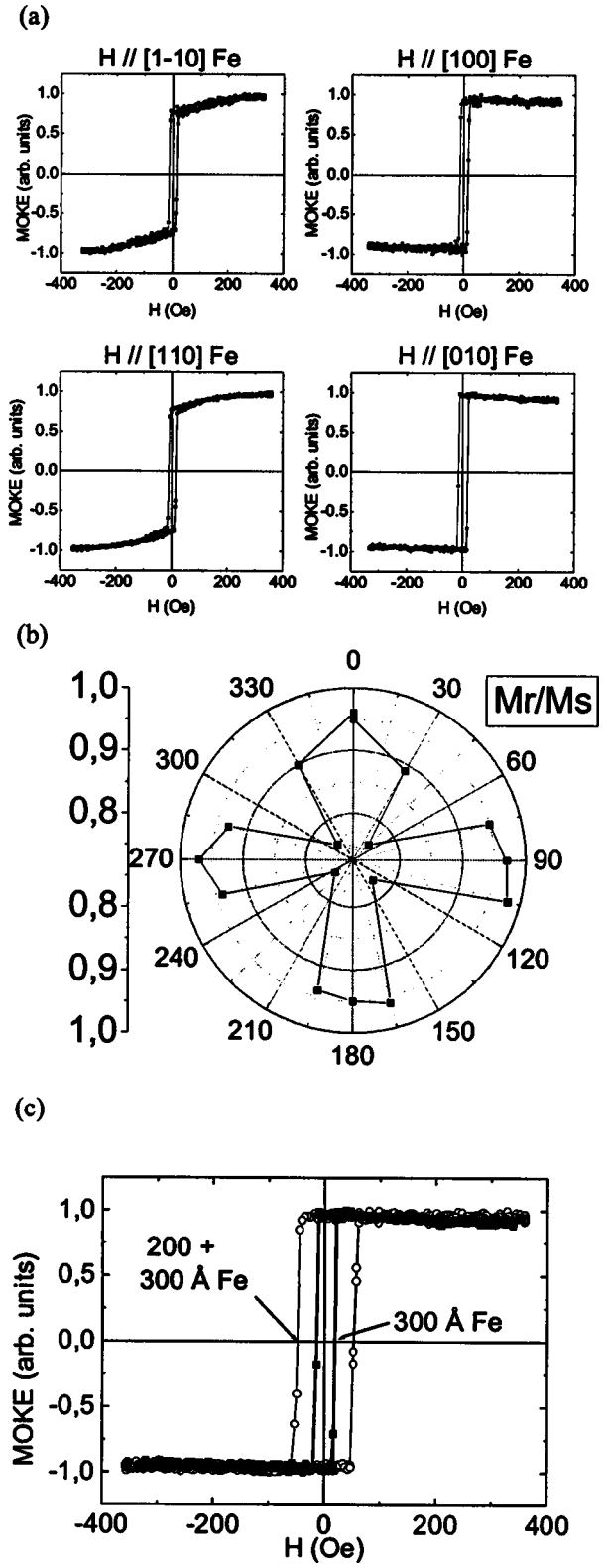

FIG. 4. (a) Normalized hysteresis loops with the magnetic field applied along different in-plane directions for a single 300 Å Fe layer on a MgO/Si(001) substrate. (b) Polar plot showing M_r/M_s vs the applied field angle. (c) Hysteresis loops of 300 and 500 Å Fe along the [100] direction, showing the difference in coercive fields.

ercive fields of the order of 50 Oe, as shown in Fig. 4(c) where hysteresis loops along the [100] direction are shown for both single and double layer Fe samples. This increase in coercivity may be associated with the increase in roughness

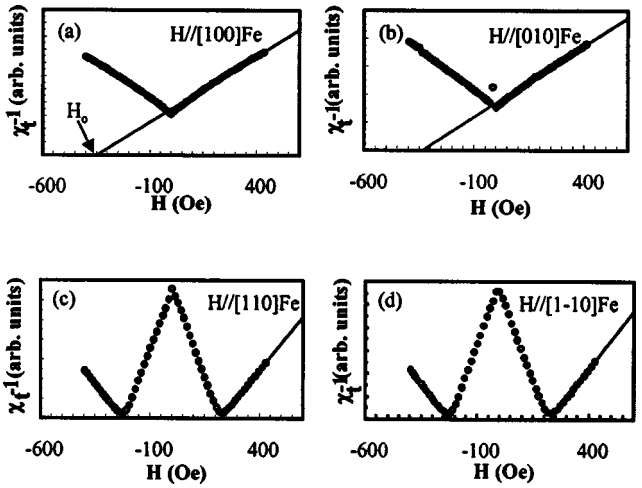

FIG. 5. Experimental inverse of the transverse susceptibility and linear extrapolation as a function of the magnetic field for the single Fe layer structure. *H* applied along (a) [100]; (b) [010]; (c) [110]; and (b) [1-10] Fe directions.

morphology which would lead to an increase in the number of pinning centers for domain wall movement.[41]

In the two cases presented there has been no evidence of the in-plane uniaxial anisotropy often found in the same Fe/MgO and other similar systems mentioned before. Being this additional anisotropy commonly attributed to an interfacial origin, the poor quality of the first MgO film on top of which the Fe layer is grown would explain the absence of this anisotropy. For further confirmation of the presence or absence of this uniaxial anisotropy, the availability of a sufficiently sensitive technique like TBIS and a formalism that allows quantification of the values and precise directions of the magnetic anisotropies would be very helpful.[33] This is due to the fact that, while the hysteresis loop is represented as M vs H, the TBIS is depicted as dM/dH vs H, and any small change in M may have significant consequences on dM/dH. In Fig. 5 we show the inverse of the transverse susceptibility χ_t^{-1} as a function of H for the magnetic field applied along the [100] and [010] easy directions of the single Fe layer. Linear extrapolations for high H values are also shown. In order to estimate the effective anisotropy constant $K_{\text{eff}} = H_0 M_s/2$ a value of $M_s \approx 1700$ emu/cc was used, where H_0 [010] and H_0 [100] are cuts in the abscissa in the corresponding linear extrapolations.[33] The difference between H_0 [010] and H_0 [100] ($\approx$5%), not observable from the polar plot in Fig. 4, could be indicative of superimposed weak uniaxial in-plane anisotropy. Essentially, H_0 [010]$-H_0$ [100]$=2H_1 r \cos 2\alpha$, with $r=K_u/K_1$ being the ratio between the fourfold anisotropy constant K_1 and the uniaxial anisotropy constant K_u, H_1 the pure fourfold anisotropy field, and α the angle between the [010] direction and the uniaxial anisotropy easy axis direction.[33] At first, it is surprising that extremely low anisotropies affect magnetization reversal. However, when the magnetization process occurs by domain wall displacement, the additional uniaxial anisotropy, even though it is small compared with the biaxial anisotropy, can significantly affect the reversal mechanism. In contrast, once the sample has been saturated along a hard

Downloaded 11 Jun 2010 to 161.116.168.169. Redistribution subject to AIP license or copyright; see http://jap.aip.org/jap/copyright.jsp

axis, magnetization reversal involves complicated magnetization rotation. Examples of inverse of transverse susceptibility and linear extrapolations with field H applied along Fe hard axes of this single Fe layer structure are shown in Fig. 5.

With regard to the double Fe layer structure, the measured TBIS curves are qualitatively similar to those obtained for the 300 Å film, with anisotropy values along the [100] and [010] directions of 3.8 and 3.9×10^5 erg/cc, respectively, slightly higher than the values found for the single Fe layer film but still evidence of the presence of small additional uniaxial anisotropy in this structure. Goryunov *et al.* have found a similar thickness dependent magnetic anisotropy in the Fe/MgO(001) system in the same Fe thickness range[42] that approached the bulk values as the films became increasingly thicker and interpreted their findings as a combination of volume plus surface anisotropy. This surface anisotropy could be induced by strain at the film/substrate interface, and would gradually be less important as the film gets thicker due to strain relaxation.

V. MAGNETIC PROPERTIES OF Fe/MgO MULTILAYERS

Due to the optical character of the MOKE technique, interpretation of the hysteresis loops from a metal/insulator multilayered structure is not as straightforward as that for an individual ferromagnetic film. In that case, the variation of the reflectivity of light polarized in the plane of incidence would be a weighted sum of the MOKE for each magnetically active layer, taking into consideration both light interference and attenuation for every layer. As a consequence, the signal detected is mostly due to the uppermost layers, but also depends in a complicated manner on the individual layer thicknesses and incidence angles. It is therefore necessary to model the magneto-optical response of such a system by use of transfer matrix formalism.[43,44] Applying this formalism to the Fe/MgO multilayered structure discussed in this work, we find that magnetization reversal of the bottom Fe layer will produce a reduction of only 4% of the total MOKE signal with respect to saturation. On the other hand, the contribution by the medium (200 Å Fe) and top (100 Å Fe) layers will be almost equivalent, with the lower thickness of the latter being compensated for by its proximity to the surface. Therefore, in this particular experiment we are mainly sensitive to the topmost Fe layers.

Taking these considerations into account, a set of low-field MOKE loops were recorded, as shown in Fig. 6, for a variety of magnetic field orientations relative to the crystallographic axes of the multilayered structure. When field is applied along the easy [100] and [010] Fe directions, only a clear Barkhausen jump is noticeable. On the other hand, in applying the magnetic field along the [110] and [−110] hard axes magnetization proceeds via an irreversible jump plus reversible rotation. For intermediate directions, such as those labeled 30°, 75°, 120° and 165°, in Fig. 6 magnetization reversal does not occur in a single step, but in two and sometimes three distinct processes that can be explained either as due to intermediate states in a Fe single layer[30,34] or to individual magnetization reversal of each Fe layer. Bearing in mind the enhanced crystalline quality of the Fe layers throughout the structure, we anticipate that each Fe layer has somewhat dissimilar coercive (H_c) and anisotropy fields (H_{eff}).[45,46]

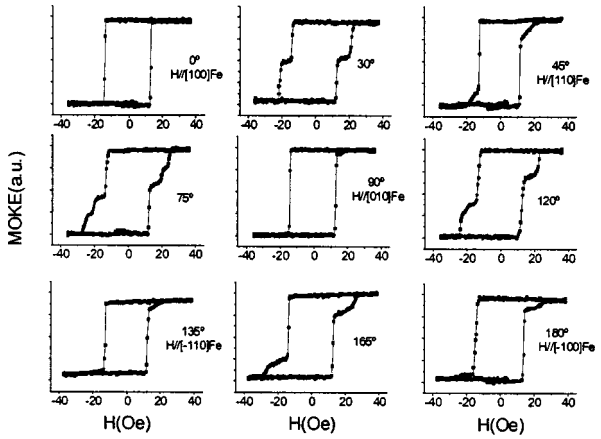

FIG. 6. Azimuthal dependence of minor hysteresis loops of the Fe/MgO multilayered structure.

As a result of disparities in the magnetization reversal processes, domain wall propagation for magnetic easy axes, and magnetization rotation for hard axes, the three Fe layers would all reverse together when the magnetic field is applied along the easy axes because of domain wall stray field induced coupling.[47] Conversely, applying the magnetic field along any other direction Fe layers would involve rotations and therefore no coupling due to domain wall stray fields. As a consequence, each individual Fe layer would more likely reverse its magnetization independently.

To clarify this, in Fig. 7 we show TBIS experiments performed in this kind of structure. Let us remind the reader that, when the magnetic field is applied along a hard axis, a minimum is observed in the inverse of the transverse susceptibility at a value of the magnetic field above which the film is saturated.[29] The value of this field can be estimated as $H_{\text{sat}}=H_1(1-r\sin 2\alpha)$.[33] The occurrence of multiple minima in the χ_t^{-1} vs H curves in Figs. 7(c) and 7(d) can be ex-

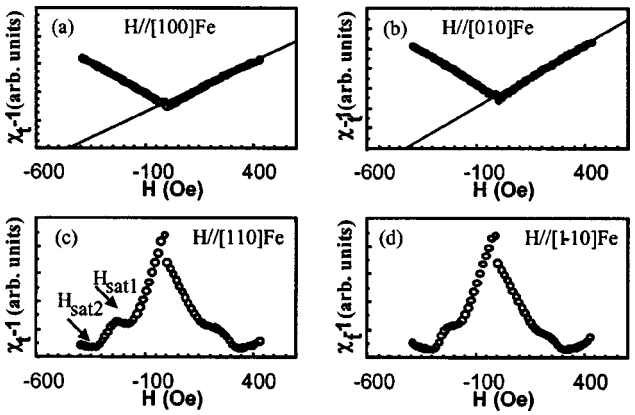

FIG. 7. Experimental inverse of the transverse susceptibility of a magnetic trilayer consisting of 100, 200 and 300 Å Fe layers separated by 20 Å MgO barriers. (a) H applied along the [100]Fe, (b) [010]Fe, (c) [110]Fe and (d) [1-10]Fe directions. Linear extrapolations along the easy axes are also shown.

Downloaded 11 Jun 2010 to 161.116.168.169. Redistribution subject to AIP license or copyright; see http://jap.aip.org/jap/copyright.jsp

TABLE I. Cuts with the abscissa H_0 extrapolated from the inverse of the transverse susceptibility at high fields applied along [100] and [010], and calculated effective anisotropy constant K_{eff} for three types of samples grown on Si(001). Bulk Fe fourfold anisotropy constant $K_1 = 4.8 \times 10^5$ erg/cc.

Total amount of Fe (Å)	H_0 [100] (Oe)	K_{eff} [100] (erg/cc)	H_0 [010] (Oe)	K_{eff} [010] (erg/cc)
300 (single layer)	333	3.6×10^5	352	3.8×10^5
500 (single layer)	350	3.8×10^5	364	3.9×10^5
600 (trilayer)	430	4.7×10^5	450	4.9×10^5

plained by the presence of two magnetic phases that are weakly coupled. The two regions show two different H_{sat} values, $H_{sat2} = 330$ Oe and $H_{sat1} = 195$ Oe, corresponding to magnetically independent regions with different H_1 values. The observation of only two phases can be explained by the small signal from the bottom Fe layer, and therefore being mostly sensitive to the two top ones. Another possible reason would be the presence of pinholes in one of the MgO spacers; this would exchange couple two Fe layers that would therefore behave as a unique ferromagnetic entity, but this possibility was ruled out by the TEM results.

Table I shows a compilation of the anisotropy constants obtained by TBIS for the three samples as well as for the Fe bulk value. One clear trend is the increase in anisotropy constant towards the bulk value as the total amount of Fe in the different samples increases. There are some possible reasons with which to explain this: roughness, Fe oxide formation localized at the very interfacial region with reduced magnetization and anisotropy,[48,49] or magnetoelastic effects via lattice distortion that would relax as the film gets thicker.[42] Since the trilayered sample (the one with the greatest number of interfaces) with a total amount of Fe of 600 Å has a K_{eff} value closer to that of bulk Fe, oxide formation at the interfaces does not seem to play an important role in reducing the anisotropy constant. Rather, strain relaxation seems to be a more plausible explanation since, upon layer accumulation in the multilayered structure, film strain would relax from the generation of dislocations at the interfaces.[50]

VI. CONCLUSIONS

We have studied the epitaxy, magnetization reversal and magnetic anisotropy in single layer and multilayered Fe/MgO structures grown on Si(001) substrates. Despite the low crystalline quality of the first MgO grown on Si, it improves after successive deposition of Fe and MgO layers by gradual lattice accommodation through the reduced misfit between layers. The influence of the initial buffer morphology hinders observation of the commonly observed in-plane uniaxial magnetic anisotropy by Kerr loops. This is nevertheless detected by more sensitive TBIS experiments.

Growth of Fe single layers in two steps, first at RT plus annealing, and second at high temperature, gives rise to increased morphology roughness, which in turn affects magnetization reversal by the observed enhancement in coercive field.

With respect to the multilayered structures, any conclusion reached from magneto-optical characterization is affected by the difference in sensitivity to the successive Fe layers, making any interpretation nontrivial. Two instead of three different magnetic phases are concluded from TBIS experiments on this structure. The low sensitivity to the bottom Fe layer or the presence of pinholes in the MgO spacer that could couple ferromagnetically different Fe films could explain this effect.

Finally, the anisotropy constant is found to gradually increase towards the bulk value in different samples as the total amount of Fe increases, probably due to strain relaxation as the film gets thicker.

ACKNOWLEDGMENTS

This work was performed through financial support by the Spanish Commission of Science and Technology. The authors thank E. Navarro for the AFM measurements, and J. L. Costa-Krämer for fruitful discussions. One of the authors (C.M.B.) acknowledges the Ministerio de Ciencia y Tecnología for funding.

[1] G. A. Prinz, Science **282**, 1660 (1998).
[2] J. F. Gregg, I. Petej, E. Jouguelet, and C. Dennis, J. Phys. D **35**, R121 (2002).
[3] M. T. Johnson, P. J. H. Bloemen, F. J. A. den Broeder, and J. J. de Vries, Rep. Prog. Phys. **59**, 1409 (1996).
[4] J. R. Waldrop and R. W. Grant, Appl. Phys. Lett. **34**, 630 (1979).
[5] G. A. Prinz and J. J. Krebs, Appl. Phys. Lett. **39**, 397 (1981).
[6] J. J. Krebs, B. T. Jonker, and G. A. Prinz, J. Appl. Phys. **61**, 2596 (1987).
[7] C.-A. Chang, J. Vac. Sci. Technol. A **9**, 98 (1991).
[8] M. Tonouchi, Y. Sakaguchi, and T. Kobayashi, J. Appl. Phys. **62**, 961 (1987).
[9] D. K. Fork, F. A. Ponce, J. C. Tramontana, and T. H. Geballe, Appl. Phys. Lett. **58**, 2294 (1991).
[10] K. Nashimoto, D. K. Fork, and T. H. Geballe, Appl. Phys. Lett. **60**, 1199 (1992).
[11] W. H. Lee *et al.*, Appl. Phys. Lett. **77**, 2192 (2000).
[12] T. Ishiguro, Y. Hiroshima, and T. Inoue, Jpn. J. Appl. Phys., Part 1 **35**, 3537 (1996).
[13] P. A. Stampe and R. J. Kennedy, Thin Solid Films **326**, 63 (1998).
[14] A. Masuda, Y. Yamanaka, M. Tazoe, Y. Yonezawa, A. Morimoto, and T. Shimizu, Jpn. J. Appl. Phys., Part 1 **34**, 5154 (1995).
[15] X. Y. Chen, B. Yang, Z. G. Liu, and L. J. Shi, Appl. Surf. Sci. **135**, 233 (1998); X. Y. Chen, K. H. Wong, C. L. Mak, X. B. Yin, M. Wang, J. M. Liu, and Z. G. Liu, J. Appl. Phys. **91**, 5728 (2002).
[16] H. Shimakage, A. Kawakami, and Z. Wang, IEEE Trans. Appl. Supercond. **9**, 1645 (1999); J.-G. Yoon, H. K. Oh, and S. J. Lee, Phys. Rev. B **60**, 2839 (1999); F. Niu, B. H. Hoerman, and B. W. Wessels, Appl. Surf. Sci. **161**, 74 (2000).
[17] T. Kanaji, K. Asano, and S. Nagata, Vacuum **23**, 55 (1973).
[18] T. Kanaji, T. Kagotani, and S. Nagata, Thin Solid Films **32**, 217 (1976).
[19] C. Li *et al.* Phys. Rev. B **43**, 780 (1991).
[20] Y. V. Goryunov *et al.*, J. Appl. Phys. **76**, 6096 (1994).
[21] Y. V. Goryunov, N. N. Garifyanov, G. G. Khaliullin, I. A. Garifullin, L. R. Tagirov, F. Schreiber, Th. Mühge, and H. Zabel, Phys. Rev. B **52**, 13450 (1995).
[22] Y. Park, E. E. Fullerton, and S. D. Bader, Appl. Phys. Lett. **66**, 2140 (1995).
[23] J. H. Wolfe, R. K. Kawakami, W. L. Ling, Z. Q. Qui, R. Arias, and D. L. Mills, J. Magn. Magn. Mater. **232**, 36 (2001).
[24] O. Durand, J. R. Childress, P. Galtier, R. Bisaro, and A. Schuhl, J. Magn. Magn. Mater. **145**, 111 (1995).
[25] L. Abelmann and C. Lodder, Thin Solid Films **305**, 1 (1997).
[26] M. Bowen *et al.*, Appl. Phys. Lett. **79**, 1655 (2001).

Downloaded 11 Jun 2010 to 161.116.168.169. Redistribution subject to AIP license or copyright; see http://jap.aip.org/jap/copyright.jsp

[27] E. Popova *et al.*, Appl. Phys. Lett. **81**, 1035 (2002).
[28] J. Faure-Vincent, C. Tiusan, C. Bellouard, E. Popova, M. Hehn, F. Montaigne, and A. Schuhl, Phys. Rev. Lett. **89**, 107206 (2002).
[29] C. Contreras, J. L. Menéndez, A. Cebollada, and J. F. Calleja, Jpn. J. Appl. Phys., Part 1 **38**, 6699 (1999).
[30] J. L. Costa-Krämer, J. L. Menéndez, A. Cebollada, F. Briones, D. García, and A. Hernando, J. Magn. Magn. Mater. **210**, 341 (2000).
[31] C. Martínez Boubeta, E. Navarro, A. Cebollada, F. Briones, F. Peiró, and A. Cornet, J. Cryst. Growth **226**, 223 (2001).
[32] C. Martínez Boubeta *et al.*, Surf. Sci. **482**, 910 (2001).
[33] J. F. Calleja, J. L. Menéndez, A. Cebollada, and C. Contreras, Jpn. J. Appl. Phys., Part 1 **40**, 6829 (2001).
[34] F. Cebollada, A. Hernando-Mañeru, A. Hernando, C. Martínez Boubeta, A. Cebollada, and F. González, J. M. Phys. Rev. B **66**, 174410 (2002).
[35] K. Arima, K. Endo, T. Kataoka, Y. Oshikane, H. Inoue, and Y. Mori, Appl. Phys. Lett. **76**, 463 (2000).
[36] D. Berling *et al.*, J. Magn. Magn. Mater. **191**, 331 (1999).
[37] C. Liu, Y. Park, and S. D. Bader, J. Magn. Magn. Mater. **111**, L225 (1992).
[38] K. Thürmer, R. Koch, M. Weber, and K. H. Rieder, Phys. Rev. Lett. **75**, 1767 (1995).
[39] F. Family and J. G. Amar, Mater. Res. Soc. Symp. Proc. **528**, 93 (1998).
[40] D. Berling, P. Bertoncini, A. Mehdaoui, P. Wetzel, G. Gewinner, and B. Loegel, J. Magn. Magn. Mater. **237**, 181 (2001).
[41] A. Moschel, A. Zangwill, R. A. Hyman, and M. D. Stiles, Phys. Rev. Lett. **77**, 3653 (1996).
[42] Y. V. Goryunov, N. N. Garifyanov, G. G. Khaliullin, I. A. Garifullin, L. R. Tagirov, F. Schreiber, Th. Mühge, and H. Zabel, Phys. Rev. B **52**, 13450 (1995).
[43] J. Zak, E. R. Moog, C. Liu, and S. D. Bader, Phys. Rev. B **43**, 6423 (1991).
[44] J. L. Menéndez, Doctoral thesis, Universidad de Oviedo, Spain, 2001.
[45] J. W. Freeland, Appl. Phys. Lett. **76**, 2603 (2000).
[46] N. Inaba, A. Nakamura, T. Yamamoto, Y. Hosoe, and M. Futamoto, J. Appl. Phys. **79**, 5354 (1996).
[47] L. Thomas, M. G. Samant, and S. S. Parkin, Phys. Rev. Lett. **84**, 1816 (2000).
[48] H. L. Meyerheim, R. Popescu, J. Kirshener, N. Jedrecy, M. Sauvage-Simkin, B. Heinrich, and R. Pinchaux, Phys. Rev. Lett. **87**, 076102 (2001).
[49] H. L. Meyerheim, R. Popescu, N. Jedrecy, M. Vedpathak, M. Sauvage-Simkin, R. Pinchaux, B. Heinrich, and J. Kirshener, Phys. Rev. B **65**, 144433 (2002).
[50] P. Bertoncini, D. Berling, P. Wetzel, A. Mehdaoui, B. Loegel, G. Gewinner, C. Ulhaq-Bouillet, and V. Pierron-Bohnes, Surf. Sci. **454–456**, 755 (2000).

Downloaded 11 Jun 2010 to 161.116.168.169. Redistribution subject to AIP license or copyright; see http://jap.aip.org/jap/copyright.jsp